Journal of Applied Polymer Science

Formula and process optimization of controlled-release microcapsules prepared using a coordination assembly and the response surface methodology

BeiXing Li,[1,2] Lei Guan,[1] Kai Wang,[1] DaXia Zhang,[1,2] WeiChang Wang,[1] Feng Liu[1]

[1]Key Laboratory of Pesticide Toxicology & Application Technique, Department of Plant Protection, Shandong Agricultural University, Tai'an Shandong, People's Republic of China

[2]Research Center of Pesticide Environmental Toxicology, Shandong Agricultural University, Tai'an Shandong People's Republic of China

Correspondence to: F. Liu (E-mail: fliu@sdau.edu.cn)

ABSTRACT: A model chlorpyrifos microcapsule was prepared using coordination assembly between Fe^{3+} and tannic acid (TA). The influence of independent variables such as the dropping rate of TA (X_1) and Fe^{3+} (X_3), the concentration of TA (X_2) and Fe^{3+} (X_4), and the reaction temperature (X_5) on the encapsulation efficiency (R_1) and release characteristics (R_2) of the microcapsule had been investigated, based on a central composite design with five factors and five levels. The results showed that the main factors influencing R_1 and R_2 were X_4 and X_2, then the interaction between X_2 and X_4, followed by X_5 and X_3. The optimal formula mainly based on higher R_1 and lower R_2 were determined and then tested. The optimized conditions led to an encapsulation efficiency and cumulative release proportion of 97.12% ± 0.72% and 40.07% ± 0.53%, along with the average relative errors of predicted values being 1.78% and −1.60%, respectively. © 2015 Wiley Periodicals, Inc. J. Appl. Polym. Sci. **2016**, *133*, 42865.

KEYWORDS: inorganic polymers; self-assembly; synthesis and processing

Received 18 April 2015; accepted 23 August 2015
DOI: 10.1002/app.42865

INTRODUCTION

Microencapsulation has been a promising approach by which we can encapsulate an active ingredient or living biomaterials to achieve controlled release. Significant advances have been observed in the food industry,[1–5] chemical materials,[6–10] pharmaceuticals,[11–13] biomaterials,[14–18] and other fields over the last decades. There are numerous encapsulation methods, including *in-situ* polymerization,[19–22] interfacial polymerization,[23–26] simple and complex coacervation,[27–30] spray drying,[31–35] solvent evaporation,[36–38] and so on. The *in-situ* polymerization has received extensive application on account of the inexpensive membrane materials and simple manufacturing equipments.[19] However, it is a highly complex procedure that requires professional staff when it is applied to industrial applications. Formaldehyde is one of the most important precursors for a membrane material used for *in-situ* polymerization, but it has a pungent smell and high toxicity for higher animal life.[39–41] Interfacial polymerization is a promising technique that requires relatively simple process parameters and lower emphasis on monomer purity than conventional methods.[42] But it too has a few shortcomings, such as being time-consuming, the high cost of monomer, and so on. Biocompatible materials are usually adopted when considering complex coacervation. These are favorable for environment protection and they also have a low mammalian toxicity.[43] However, encapsulation efficiency is a very important parameter that should not be neglected, and microcapsules prepared via complex coacervation possess very low encapsulation efficiency.[44] Spray drying and solvent evaporation are both low-cost and simple methods, but the former exhibits a drawback similar with complex coacervation, while the latter is less likely to possess a high drug-loading efficiency.[34–37]

A one-step assembly of coordination complexes has stimulated significant interest among scientists in the recent years due to its simplicity and convenience. Ejima *et al.*[45] have prepared Fe^{3+}–tannic acid (TA) films both on planar and solid particles by deposition of TA and Fe^{3+}. Bentley *et al.*[46] introduced other self-assemblers, namely phenolics (caffeic acid), gallic acid, catechol (dopamine), and flavones. TA is a natural polyphenol with 10 ester groups. It could therefore be regarded as the esterified

Additional Supporting Information may be found in the online version of this article.

Table I. The Level Table for Experimental Factors

	Level				
Factor	−2.378	−1.000	0.000	1.000	2.378
X_1: dropping rate of TA/μmol min^{-1} mL^{-1}	0.1685	0.4115	0.5879	0.7643	1.007
X_2: total concentration of TA/μmol mL^{-1}	0.7313	4.703	7.055	9.406	12.65
X_3: dropping rate of Fe^{3+}/μmol min^{-1} mL^{-1}	0.4007	0.8929	1.250	1.607	2.100
X_4: total concentration of Fe^{3+}/μmol mL^{-1}	1.209	9.821	16.07	22.32	30.93
X_5: reaction temperature/°C	21.22	35.00	45.00	55.00	68.78

product of a reaction among several gallic acid molecules.[47] TA and Fe^{3+} are organic ligands and inorganic cross-linkers, respectively. A stable octahedral complex is obtained from the reaction between three of the galloyl groups of TA and Fe^{3+} ion.[48] Ejima *et al.*[45] reported that the reaction was analogous to layer-by-layer assembly and the thickness of the formed membrane could be further increased by repeating the deposition process, during which the reaction might be influenced by the addition rate of TA and Fe^{3+} ion. However, encapsulation technology of this coordination assembly method had not been reported previously based on organic phase. There are significant differences in terms of the interfacial properties of liquid–liquid interface and solid–liquid interface, thus the deposition process of TA–Fe^{3+} might be different. Therefore, it is of great significance to definitize and optimize the deposition process based on organic–aqueous interface. Pesticide microcapsules were always prepared using liquid technical material or by dissolving solid technical material in appropriate solvent before the deposition process; thus, the deposition on this kind of interface was appropriate to be selected as a model.

Response surface methodology (RSM), a useful method to clarify how several factors influenced the responses, was one of the most typical designs of experiment.[49–55] Among them, central composite design was the most commonly used second-order design.[56–58] As a proof, attempts were made to optimize both the encapsulation efficiency and the release characteristics of microcapsules prepared using coordination assembly. A model chlorpyrifos microcapsule was prepared by means of the response surface method and the influences of several main factors on the two indexes were analyzed.

MATERIAL AND METHODS

Materials

Chlorpyrifos (purity >97%) was purchased from Jiangsu Baoling Chemical Co. (Jiangsu, China) for the preparation of microcapsules. Xylene was purified as a solvent for microcapsules. TA ($C_{76}H_{52}O_{46}$, AR) and iron (III) chloride hexahydrate ($FeCl_3{\cdot}6H_2O$, ACS) were all purchased from Aladdin Reagent Co. (Shanghai, China). Polyoxyethylene castor oil ether (EL-40, nonionic surfactant) was purchased from Jiangsu Hai'an Petrochemical Plant (Jiangsu, China) and was used as an emulsifier. Distilled water was used throughout the study.

Preparation of Microcapsule

The standard procedure used is described as follows: in the first step, 10 g chlorpyrifos and 3 g xylene were mixed to obtain a homogenous organic phase while 1 g EL-40 was dissolved in 40 mL water. Then the organic phase was added to the aqueous continuous phase. Homogenization required the use of a homogenizer at 10,000 r/min at this time. The emulsion was stirred at 1200 r/min at room temperature after having been transferred to a three-neck flask. Solutions of $FeCl_3{\cdot}6H_2O$ and TA were then added to yield their final concentrations. The dropping rates of Fe^{3+} (calculated by the mass of the iron ion, also conducted below) and TA, the total concentration of Fe^{3+} and TA, and the reaction temperature were determined according to the proposed experiments (Table S1, Supporting information). After the coordination reaction, the mixture was centrifuged at 3000 r/min for 10 min, and the supernatant was removed. The particles were washed three times to remove excess TA and Fe^{3+}. Finally, the resultant microcapsules were dried in a vacuum oven for 96 h (drying temperature: 30°C; vacuum degree: 133 Pa).

Response Surface Methodology

The experiments in the current work were designed using the software Design Expert 8.05 (Stat-Ease, Minneapolis, USA), which required five levels coded as (−2.378), (−1), (0), (+1), and (+2.378). Full designs were performed with one block and ten center points using five factors at five levels (Table I). The data analysis and model building were also performed using the same software.

Encapsulation Efficiency Measurement

In terms of the encapsulation efficiency measurement, there were numerous methods. To simplify the process, we adopted a published method.[59] A total of 0.2 g microcapsule suspension was accurately weighed on an analytical balance (±0.0001 g; Sartorius; Goettingen, Germany), and then transferred to a 100 mL beaker. Then 15 mL decane was added and the dispersion was shaken at 300 times/min for 3 min to dissolve the active ingredient that remained outside the microcapsules. Subsequently, the dispersion was centrifuged at 3000 r/min for 5 min. Finally, the upper layer of the solution which contains the unencapsulated chlorpyrifos (m_{out}) was analyzed by gas chromatography (GC). In terms of the determination of the total weight of chlorpyrifos in the 0.2 g microcapsule suspension (m_{to}), the initial procedures were in accordance with the measurement of m_{out}. The only difference was that samples were treated with an ultrasonic cell crusher before centrifugation.[60] The details of the GC is described as follows: The GC system (GC-2010plus; Shimadzu; Kyoto, Japan) was equipped with a nonpolar capillary column (Rtx-5; 30 m × 0.32 mm ID × 0.25

Table II. Fitness of the Encapsulation Efficiency to Different Models

Model	Sequential *P*-value	Lack of fit (*P*-value)	Adjusted R^2	Predicted R^2
Linear	<0.0001	0.0025	0.9641	0.9568
Two-factor interaction	<0.0001	0.0087	0.9848	0.9851
Quadratic polynomial	<0.0001	0.1646	0.9982	0.9957
Cubic polynomial	0.0373	0.3821	0.9992	0.9915

μm film thickness; Restek, Bellefonte, USA), coated with 5% diphenyl and 95% dimethylpolysiloxane. Nitrogen (99.99% purity) was used as carrier gas at a constant flow rate of 60 mL/min. Analysis was carried out with the injection port set at 260°C, the detector (flame photometric detector, FPD) 260°C, and the oven temperature fixed at 230°C. The measurements were repeated in triplicate. Encapsulation efficiency was calculated using eq. (1):

$$\text{Encapsulation efficiency}\,(\%) = (1 - m_{out}/m_{to}) \times 100 \quad (1)$$

where m_{out} and m_{to} are the weight of chlorpyrifos outside the microcapsules and the total weight of chlorpyrifos in the 0.2 g microcapsule suspension, respectively.

Release Characteristics of Microcapsule

In all, 0.2 g dried microcapsule sample was accurately weighed and then transferred to a 250-mL three-necked flask with a stirrer in a water bath at 30°C. A stirring rate of 500 r/min was used, and 60 mL methanol and 140 mL distilled water were mixed and used as a release medium. Subsequently, 2 mL liquid was removed at 4 h to measure the weight of chlorpyrifos in it, and then, its total content in the mixture was calculated (m_2). The weight of chlorpyrifos in 0.2 g dried microcapsule (m_3) was also determined by GC. The cumulative release proportion (4 h) was calculated using the following eq. (2):

$$\text{Cumulative release proportion}\,(\%) = (m_2/m_3) \times 100 \quad (2)$$

RESULTS AND DISCUSSION

The RSM design matrix and two corresponding responses are presented as the means ± SD (Table S1, Supporting information). Apparently, the responses of experimental runs differed significantly. To be specific, the encapsulation efficiency (R_1) ranged between 28.09% and 94.37%. In terms of cumulative release proportion (R_2), the tendency was almost the opposite compared with that of R_1. The samples with higher R_1 always exhibited controlled release. In the current study, we expected to generate a preparation with higher R_1 and lower R_2. Therefore, the data for the two responses were analyzed to obtain an optimized formula that meets the above criteria.

Statistical Analysis of Encapsulation Efficiency

A regression analysis was performed to fit the responses with the experimental data using the Design-expert software. Linear, two-factor interaction, quadratic, and cubic polynomial models were selected to test the fitness of encapsulation efficiency, respectively. It was apparent that the higher the "adjusted R^2" and the "predicted R^2" were the better the fit. As shown in Table II, the values for the "Adjusted R^2" of the cubic model were the highest for two responses; however, the model was aliased according to the Design-Expert software. The "lack of fit *P*-value" revealed whether the "lack of fit" is significant relative to the pure error or not. The data of R_1 was fitted best to the quadratic polynomial model, with the "lack of fit *P*-value" of 0.1646, implying that it was applicable models. Previous publications indicated that quadratic polynomial model was more appropriate to fit the responses of multifactor experiments when the interactions were taken into account.[61] It was also demonstrated in the current study. The quadratic polynomial model can be defined as:[52,62]

$$Y = b_0 + \sum_{i=1}^{5} b_i \times X_i + \sum_{i=1}^{5} b_{i,j} \times X_i \times X_j + \sum_{i=1}^{5} b_{i,i} \times X_i^2 \quad (3)$$

where Y is the encapsulation efficiency, b_0 term is the interception coefficient, the X_i terms are the investigated factors and the b_i, $b_{i,j}$, $b_{i,i}$ terms are the related equation coefficients.[49]

The analysis of variance (ANOVA) for the RSM polynomial model was then conducted based on Fischer tests and used to indicate the adequacy of the fitted model with the corresponding *P*-value, along with the regression equation coefficients (Table S2, Supporting information). The *F* value was a measure of the variation of data around the mean and it also indicated the relevance of the proposed model to predict the experimental results. The model *F*-value of R_1 was 1218.853, implying significant models, with only a 0.01% chance that a "Model *F*-value" this large could occur due to noise. The *P*-value was also used to determine the significance of each data, which essentially indicates a value of "Prob > *F*". Lower *P*-values indicated higher significance, and a value less than 0.05 indicated that the data were significant. The fitness of the residuals to the normal distribution is depicted in Figure 1. As for a normal plot, it was thought to be an ideal model when the points lined up along the diagonal. A significant trend of points away from the diagonal indicated an abnormal distribution, implying significant sources of error that could not be accounted for by random

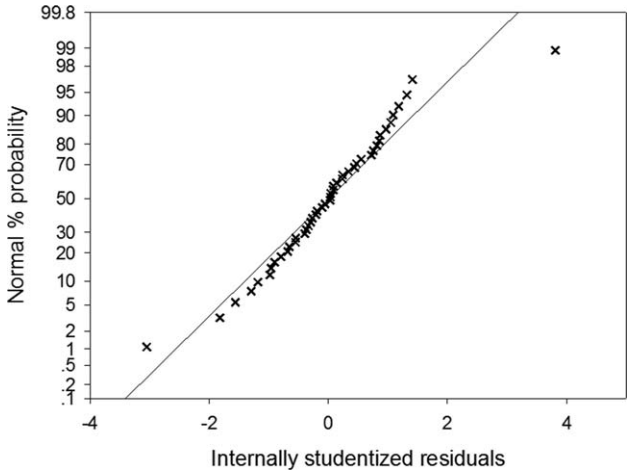

Figure 1. Normal plots of residuals for the data of encapsulation efficiency.

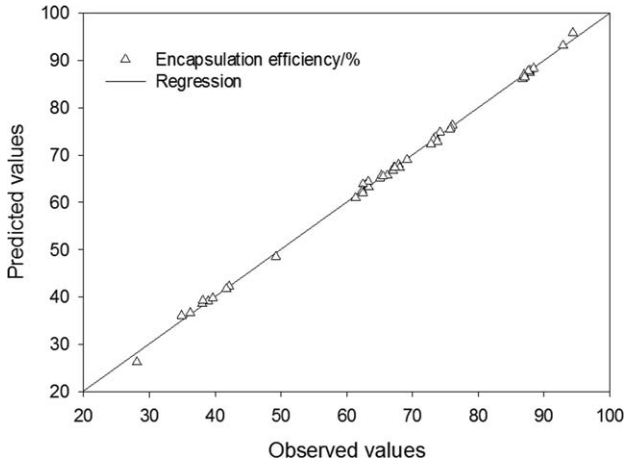

Figure 2. Observed values vs. predicted values for modeled encapsulation efficiency.

error (mainly setting error and operational error).[63] Most points in Figure 1 were fairly close to the normal. However, the points in the normal plots demonstrated a slight element of skewness, especially the points representing 39 and 40 (run number of Table S1). Therefore, a conclusion could be drawn that when total concentration of Fe^{3+} was too high or too low, the predictability of the models was reduced. The *P*-values greater than 0.05 indicated that the model terms were not significant. In this case, model reduction by removing model terms had $P > 0.05$ was the best way to improve the models,[56] leading to a simplified polynomial model equation shown as follows:

$$\begin{aligned}\text{Encapsulation efficiency}\,(\%) = {} & 67.368 - 0.266X_1 + 9.392X_2 \\ & - 0.697X_3 + 14.645X_4 - 0.951X_5 + 0.324X_2X_3 - 2.945X_2X_4 \\ & + 0.303X_2X_5 + 0.562X_3X_4 + 0.617X_2^2 - 1.118X_4^2 - 0.728X_5^2\end{aligned} \quad (4)$$

It was apparent that X_1, X_2, X_3, X_4, X_5, X_2X_3, X_2X_4, X_2X_5, X_3X_4, X_2^2, X_4^2, and X_5^2 are all significant model terms of R_1. Positive and negative values of coefficients of regression equation demonstrated that both high and low levels of the considered variables are almost optimum, respectively.[56] Predicted values were obtained after calculating coded values with eq. (4). Then the predicted responses and observed responses were regressed, as shown in Figure 2. It was indicated that the empirical model showed a good fit to the observed data and gave high value of determination coefficient ($R^2 = 0.9987$). After seeing the coefficients (Table S1, Supporting information), it was obvious that the main factors influencing R_1 were the total concentrations of Fe^{3+} (X_4) and TA (X_2), then the interaction between X_2 and X_4, followed by reaction temperature (X_5) and the dropping rate of Fe^{3+} (X_3).

The influence of the variables on the response can be evaluated by illustrating response surface plots which represented the

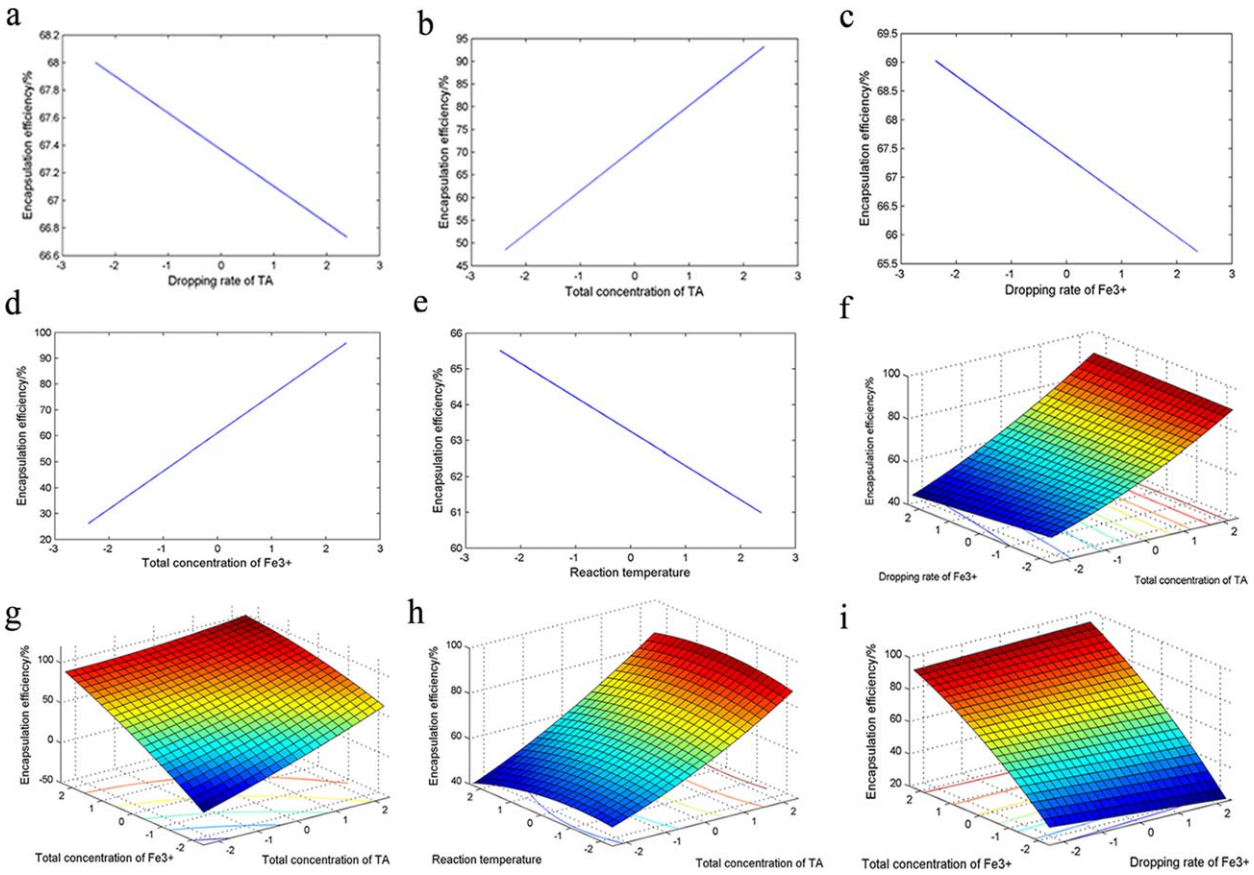

Figure 3. Response surface plots showing significant model terms of encapsulation efficiency: (a) X_1, (b) X_2, (c) X_3, (d) X_4, (e) X_5, (f) X_2X_3, (g) X_2X_4, (h) X_2X_5, and (i) X_3X_4. [Color figure can be viewed in the online issue, which is available at wileyonlinelibrary.com.]

Table III. Fitness of the Cumulative Release Proportion to Different Models

Model	Sequential *P*-value	Lack of fit (*P*-value)	Adjusted R^2	Predicted R^2
Linear	<0.0001	0.0652	0.9839	0.9807
Two-factor interaction	<0.0001	0.1802	0.9927	0.9895
Quadratic polynomial	0.5383	0.1706	0.9924	0.9824
Cubic polynomial	0.0373	0.5756	0.9977	0.9759

graphical data of the regression equation. It was one of the best methods to reveal interactions between different variables and locate the optimal level of each variable for maximal response.[64] Only significant model terms (including single factor and the interactions) of R_1 were represented in Figure 3, while maintaining the other variables at the zero level. It can be observed that an increase in the total concentration of Fe^{3+} or TA led to increasing encapsulation efficiency [Figure 3(b,d)]. However, reaction temperature, dropping rate of Fe^{3+} and TA revealed negative signs [Figure 3(a,c,e)], which indicated a reduction in R_1 when X_5, X_3, or X_1 was increased. In addition, it should be noted that several interactions also had a significant influence, especially the combinations that included X_4. Conditions with higher TA concentration and lower dropping rate of Fe^{3+} [Figure 3f)], higher concentration of TA and Fe^{3+} [Figure 3(g)], higher TA concentration and moderate reaction temperature [Figure 3(h)], moderate dropping rate of Fe^{3+}, and higher Fe^{3+} concentration [Figure 3(i)] all led to higher R_1 yields. Undoubtedly, the higher response was ascribed to the increased amount of octahedral complex, which was strongly dependent on the concentrate of TA and Fe^{3+}. However, R_1 increased less abruptly when the concentration of TA and Fe^{3+} were kept at a high level [Figure 3(g)], indicating a nearly saturated state of wall material. In this case, the excessive emphasis on the high encapsulation efficiency by increasing the amount of TA and Fe^{3+} is a waste.

Statistical Analysis of Cumulative Release Proportion

Release property is a fatal performance related to the biological activity and efficacy duration of a certain microcapsule product.[65,66] The cumulative release proportions (R_2) obtained from the RSM experiments were measured in the range of 48.55–96.00% (Table S1, Supporting information), indicating significant influence of the formula components and process variables. Statistical analysis was then conducted in order to get a formula and procedure with lower release rate because we expect to prolong the efficacy duration of chlorpyrifos microcapsule. A regression analysis was performed to fit the responses with the experimental data, when linear, two-factor interaction, quadratic, and cubic polynomial models were selected (Table III). All the four models exhibited favorable "Adjusted R^2" and "Predicted R^2" values; however, the cubic model was aliased according to Design-Expert 8.05 software. The "lack of fit" *P*-value higher than 0.05 indicates insignificant experimental error, comparing with the pure error. Apparently, the lack of fit *P*-values of linear, two-factor interaction, and quadratic polynomial models were all higher than 0.05. In terms of sequential *P*-value, however, the quadratic polynomial model was not significant. The data of R_2 was fitted best to two-factor interaction model when all the four evaluation indexes were integratedly considered. The ANOVA based on Fischer tests was conducted and the results were presented in Table S3 (Supporting information). The model *F*-value of R_2 was 406.185, implying significant models ($P < 0.0001$). It is also confirmed by Figure S1 (Supporting information), in which the fitness of the residuals to the

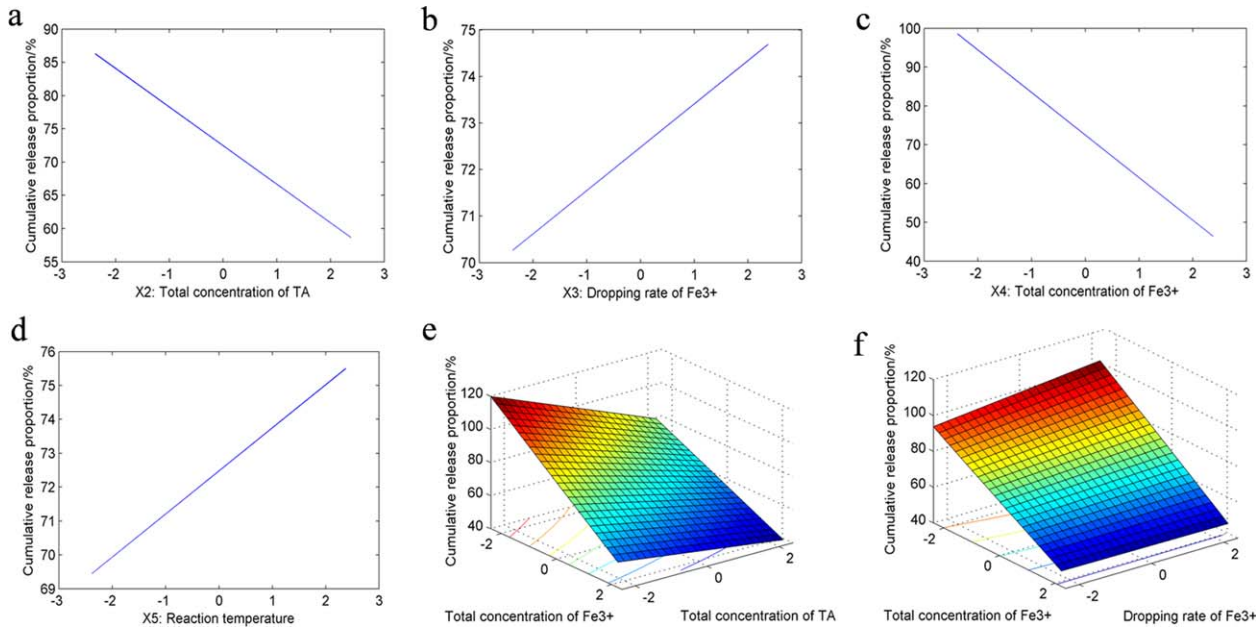

Figure 4. Response surface plots showing significant model terms of cumulative release proportion: (a) X_2, (b) X_3, (c) X_4, (d) X_5, (e) X_2X_4, and (f) X_3X_4. [Color figure can be viewed in the online issue, which is available at wileyonlinelibrary.com.]

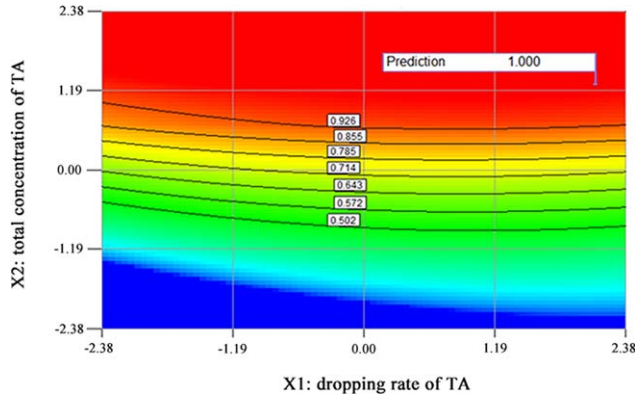

Figure 5. Desirability plot, $X_3 = 1.96$, $X_4 = 2.38$, and $X_5 = -2.32$ (coded value). [Color figure can be viewed in the online issue, which is available at wileyonlinelibrary.com.]

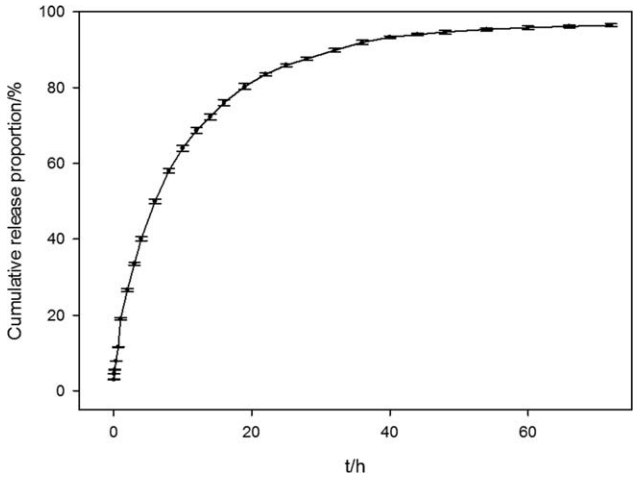

Figure 6. Release curve of chlorpyrifos-loaded microcapsules prepared under optimal conditions.

normal distribution is depicted. Most points lined up along the diagonal, indicating an ideal model with no significant sources of error that could not be accounted for by random error. Model reduction was conducted to improve the two-factor interaction model by removing the nonsignificant model terms ($P > 0.05$), leading to a simplified equation shown as follow:

$$\text{Cumulative release proportion}\,(\%) = 72.509 - 5.804X_2 + 0.930X_3 - 10.954X_4 + 1.272X_5 + 1.270X_2X_4 - 0.489X_3X_4 \quad (5)$$

From eq. (5), X_2, X_3, X_4, X_5, X_2X_4, and X_3X_4 are significant model terms of R_2. Predicted values were calculated with eq. (5) and then regressed with observed responses, displayed in Figure S2 (Supporting information). The determination coefficient R^2 equals 0.9939, indicating that only 0.61% of the variation could not be explained by the proposed model. With R_2 as the response, significant model terms were plotted while maintaining the other variables at the zero level. In response to R_2, it was almost to the contrary compared with that of encapsulation efficiency. As was shown in Figure 4(a,c), an increase in the total concentration of Fe^{3+} or TA is helpful for slowing down the release process. However, the release rate increased with the dropping rate of Fe^{3+} and reaction temperature [Figure 4(b,d)], of which we do not expect to see. Fortunately, conditions of higher concentrations of TA and Fe^{3+} [Figure 4(e)], a moderate dropping rate of Fe^{3+} and higher Fe^{3+} concentration [Figure 4(f)] both led to slower release. But it should not be ignored that when the total concentration of TA and Fe^{3+} was either high enough or low enough, the estimated values of cumulative release proportion were inaccurate according the normal plots of residuals [Figure 1(b)]. When the independent variables were maintained at the level of 2.378 or −2.378 (coded value), the estimated responses were all deflected, especially the factor of the total concentration of Fe^{3+}, the same as that shown in Figure 1.

Multiple-Response Optimization

The most important goal of applying RSM is the process optimization. To optimize the parameters with the two output responses in this work, the concept of a desirability function was employed. The total desirability was computed as a geometric mean of the individual desirability functions.[67,68] The desirability functions to obtain the maximum R_1 and the minimum R_2 were fitted by the least-squares model, while R_1 was limited from 85% to 95% and R_2 was limited from 40% to 50%. Then the level of variability that yielded the highest desirability (1.0) was selected as the optimum level. Fortunately, as many as 63 solutions were found when only the preparation technology was considered. However, we also expected to use as little TA and higher dropping rates of materials as possible due to financial and time constraints. Therefore, the integrated optimum of variables were determined as $X_1 = 2.11$, $X_2 = 1.28$, $X_3 = 1.96$, $X_4 = 2.38$, and $X_5 = -2.32$ (coded value) and the desirability was illustrated in Figure 5. The predicted values calculated according to eqs. (4) and (5) were 98.85% (R_1) and 39.43% (R_2), respectively. The microcapsule sample prepared at optimal condition was also obtained and then tested. The measured values for the sample of R_1 and R_2 were 97.12% ± 0.72% and 40.07% ± 0.53% (mean ± SD), respectively. The average relative errors of the predicted values above were 1.78% and −1.60%, respectively. Figure 6 illustrates the release curve of chlorpyrifos-loaded microcapsules prepared under optimal conditions in 30% methanol aqueous solution. The active ingredients in

Table IV. Fitness of the Release Curve of Chlorpyrifos-Loaded Microcapsules Prepared under Optimal Conditions to Different Models

Model	Mathematical expression	Empirical equation	R^2
Zero-order	$Q_t = Q_0 + K_0t$	$y = 2.571x + 21.18$	0.8314
First-order	$LnQ_t = LnQ_0 - K_1t$	$y = 0.0705x - 0.1740$	0.9808
Higuchi	$Q_t = Q_0 + K_Ht^{1/2}$	$y = 16.79x + 3.244$	0.9702

Note: Q_t is the cumulative release proportion of chlorpyrifos released at time t; Q_0, K_0, K_1 and K_H are constants.

microcapsules released fast in the first few hours. After releasing for 36 h, the cumulative release proportion of chlorpyrifos microcapsules reached 91.95% ± 0.57%. Then it increased at a relatively low rate. Besides, the active ingredient was only partly released (96.49% ± 0.36%) even after 72 hours. The curvilinear nature of the cumulative release proportion vs. time plots suggests that drug release from the microcapsule followed first-order kinetics. It is further supported by the high values of determination coefficients (R^2) obtained in modeling process. Zero-order, first-order, and Higuchi models were used to test the model fitness (Table IV). Release data were fitted best to a first-order model which yields the highest R^2 ($R^2 = 0.9808$).

CONCLUSION

Different factors that might influence the encapsulation efficiency (R_1) and release characteristic (R_2) of microcapsule prepared using coordination assembly were investigated, including the dropping rate of TA (X_1), the total concentration of TA (X_2), the dropping rate of Fe^{3+} (X_3), the total concentration of Fe^{3+} (X_4), and the reaction temperature (X_5). The RSM had been adopted for the determination of the optimal conditions for R_1 and R_2. It was found that the main factors influencing R_1 and R_2 were X_4 and X_2, and then the interaction between X_2 and X_4, followed by X_5 and X_3. The optimal condition mainly based on higher R_1 and lower R_2 was determined. A dropping rate of TA = 0.9601 μmol min^{-1} mL^{-1}, a concentration of TA = 10.06 μmol mL^{-1}, a dropping rate of Fe^{3+} = 1.950 μmol min^{-1} mL^{-1}, a concentration of Fe^{3+} = 30.94 μmol mL^{-1}, and a reaction temperature = 21.80°C led to an encapsulation efficiency and cumulative release proportion of 97.12% ± 0.72% and 40.07% ± 0.53% (mean ± SD) along with the average relative error of predicted values of 1.78% and −1.60%, respectively.

The method of coordination assembly had not been widely reported in microcapsule preparation. Our study demonstrated that it had great potential in microencapsulation, along with its speed, simplicity, and environmental friendliness. The wall material in this work was a coordination polymer prepared by the reaction between Fe^{3+} and TA. However, as was shown in the introduction, other polyphenols also had the ability to chelate with the metal ion. Whether they are capable of doing so in microencapsulation still requires further experimentation. Coordination differences of different metal ions such as Ca^{2+}, Fe^{2+}, Al^{3+}, and Cu^{2+} should also be confirmed.

ACKNOWLEDGMENTS

The authors gratefully acknowledge Ms. Wei Mu from Shandong Agricultural University for her helpful suggestions for this manuscript. The authors also honor two anonymous referees for their helpful comments for this manuscript. This work was supported by a grant from National Natural Science Foundation of China (No. 31572040) and Special Fund for Agro-scientific Research in the Public Interest from the Ministry of Agriculture of China (No. 201303027). The authors declare no competing financial interest.

REFERENCES

1. Sutter, S. C.; Buera, M. P.; Elizalde, B. E. *Int. J. Pharmaceut.* **2007**, *332*, 45.
2. Song, Y. B.; Lee, J. S.; Lee, H. G. *Colloids Surf. B: Biointerfaces* **2009**, *73*, 394.
3. Wichchukit, S.; Oztop, M. H.; McCarthy, M. J.; McCarthy, K. L. *Food Hydrocoll.* **2013**, *33*, 66.
4. Xue, F.; Li, C.; Liu, Y.; Zhu, X.; Pan, S.; Wang, L. *J. Food Eng.* **2013**, *119*, 439.
5. Faria, A. F.; Mignone, R. A.; Montenegro, M. A.; Mercadante, A. Z.; Borsarelli, C. D. *J. Agric. Food Chem.* **2010**, *58*, 8004.
6. Su, J. F.; Schlangen, E. *Chem. Eng. J.* **2012**, *198–199*, 289.
7. Xie, Z.; Chen, N.; Liu, C.; Zhou, J.; Xu, S.; Zheng, Y.; Liand, F.; Xu, Y. *Chin. J. Chem. Eng.* **2010**, *18*, 149.
8. Zhang, T.; Zhang, M.; Tong, X. M.; Chen, F.; Qiu, J. H. *J. Appl. Polym. Sci.* **2010**, *115*, 2162.
9. Zhang, M.; Gao, B.; Pu, K.; Yao, Y.; Inyang, M. *Chem. Eng. J.* **2013**, *223*, 556.
10. White, S. R.; Sottos, N. R.; Geubelle, P. H.; Moore, J. S.; Kessler, M. R.; Sriram, S. R.; Brown, E. N.; Viswanathan, S. *Nature* **2001**, *409*, 794.
11. Valente, J. F. A.; Gaspar, V. M.; Antunes, B. P.; Countinho, P.; Correia, I. J. *Polymer* **2013**, *54*, 5.
12. Wang, J.; Chen, B.; Zhao, D.; Peng, Y.; Zhuo, R. X.; Cheng, S. X. *Int. J. Pharmaceut.* **2013**, *446*, 205.
13. Hui, P. C. L.; Wang, W. Y.; Kan, C. W.; Zhou, C. E.; Ng, F. S. F.; Wat, E.; Zhang, V. X.; Chan, C. L.; Lau, C. B. S.; Leung, P. C. *Int. J. Biol. Macromol.* **2013**, *55*, 32.
14. Zhang, H.; Zhu, S. J.; Wang, W.; Wei, Y. J.; Hu, S. S. *Gene Ther.* **2007**, *15*, 40.
15. Parthasarathy, R. V.; Martin, C. R. *Nature* **1994**, *369*, 298.
16. Ma, Y.; Zhang, Y.; Wang, Y.; Wang, Q. Y.; Tan, M. Q.; Liu, Y.; Chen, L.; Li, N.; Yu, W. T.; Ma, X. J. *J. Biomed. Mater. Res. Part A* **2013**, *101A*, 1007.
17. Chang, T. M. S. *Nature* **1971**, *229*, 117.
18. Guerrero, M. P.; Bertrand, F.; Rochefort, D. *Chem. Eng. Sci.* **2011**, *66*, 5313.
19. Sukhorukov, G. B.; Antipov, A. A.; Voigt, A.; Donath, E.; Mohwald, H. *Macromol. Rapid Commun.* **2001**, *22*, 44.
20. Ma, Y.; Zhang, Y.; Zhao, S.; Wang, Y.; Wang, S. R.; Zhou, Y.; Li, N.; Xie, H. G.; Yu, W. T.; Liu, Y.; Wang, W.; Ma, X. J. *J. Biomed. Mater. Res. Part A* **2012**, *100A*, 989.
21. Su, J. F.; Wang, X. Y.; Dong, H. *Mat. Lett.* **2012**, *84*, 158.
22. Lee, H. Y.; Lee, S. J.; Cheong, I. W.; Kim, J. H. *J. Microencapsul.* **2002**, *19*, 559.
23. Dhumal, S. S.; Suresh, A. K. *Polymer* **2010**, *51*, 1176.
24. Hickey, J.; Burke, N. A. D.; Stöver, H. D. H. *J. Membr. Sci.* **2011**, *369*, 68.
25. Gaudinand Sintes-Zydowicz, F. N. *Colloids Surf. A: Physicochem. Eng. Asp.* **2011**, *384*, 698.
26. Takasu, M.; Kawaguchi, H. *Colloid Polym. Sci.* **2005**, *283*, 805.
27. Shimokawa, K.; Saegusa, K.; Wada, Y.; Ishii, F. *Colloids Surf. B: Biointerfaces* **2013**, *104*, 1.

28. Zhao, W.; Zhang, Y.; Liu, Y.; Tan, M. Q.; Yu, W. T.; Xie, H. G.; Ma, Y.; Sun, G. W.; Lv, G. J.; Zhao, S.; Ma, X. J. *J. Chem. Technol. Biotechnol.* **2013**, *88*, 449.
29. Nakagawa, K.; Nagao, H. *Colloids Surf. A: Physicochem. Eng. Asp.* **2012**, *411*, 129.
30. Weinbreck, F.; Minor, M.; Kruif, C. G. *J. Microencapsul.* **2004**, *21*, 667.
31. Wang, G.; Chen, J.; Shi, Y. *J. Food Eng.* **2013**, *117*, 82.
32. Aghbashlo, M.; Mobli, H.; Rafiee, S.; Madadlou, A. *Powder Technol.* **2012**, *225*, 107.
33. Zhang, Y.; Zhong, Q. *Food Hydrocoll.* **2013**, *33*, 1.
34. Varona, S.; Rodríguez Rojo, S.; Martín, Á.; Cocero, M. J.; Serra, A. T.; Crespo, T.; Duarte, C. M. M. *Indus. Crops Prod.* **2013**, *42*, 243.
35. dos Santos, R. C. S.; Finkler, L.; Finkler, C. L. L. *J. Microencapsul.* **2014**, *31*, 759.
36. Lee, M. H.; Hribar, K. C.; Brugarolas, T.; Kamat, N. P.; Burdick, J. A.; Lee, D. *Adv. Funct. Mater.* **2012**, *22*, 131.
37. Fan, T.; Feng, J.; Ma, C.; Yu, C.; Li, J.; Wu, X. *J. Porous Mater.* **2014**, *21*, 113.
38. Wang, Y.; Su, C. P.; Schulmerich, M.; Padua, G. W. *Food Hydrocoll.* **2013**, *30*, 487.
39. Zuev, V. V.; Lee, J.; Kostromin, S. V.; Bronnikov, S. V.; Bhattacharyya, D. *Mater. Lett.* **2013**, *94*, 79.
40. Fan, C.; Zhou, X. *Colloids Surf. A: Physicochem. Eng. Asp.* **2010**, *363*, 49.
41. Cassee, F. R.; Stenhuis, W. H.; Groten, J. P.; Feron, V. J. *Exp. Toxicol. Pathol.* **1996**, *48*, 481.
42. Wagh, S. J.; Dhumal, S. S.; Suresh, A. K. *J. Membr. Sci.* **2009**, *328*, 246.
43. Piacentini, E.; Giorno, L.; Dragosavac, M. M.; Vladisavljević, G. T.; Holdich, R. G. *Food Res. Int.* **2013**, *53*, 362.
44. Scher, H. B.; Rodson, M.; Lee, K. S. *Pesticide Sci.* **1998**, *54*, 394.
45. Ejima, H.; Richardson, J. J.; Liang, K.; Best, J. P.; van Koeverden, M. P.; Such, G. K.; Cui, J.; Caruso, F. *Science* **2013**, *341*, 154.
46. Bentley, W. E.; Payne, G. F. *Science* **2013**, *341*, 136.
47. Mori, T.; Rezai-Zadeh, K.; Koyama, N.; Arendash, G. W.; Yamaguchi, H.; Kakuda, N.; Horikoshi-Sakuraba, Y.; Tan, J.; Town, T. *J. Biol. Chem.* **2012**, *287*, 6912.
48. Ross, T. K.; Francis, R. A. *Corrosion Sci.* **1978**, *18*, 351.
49. Silva, V. B.; Rouboa, A. *Appl. Math. Comput.* **2012**, *218*, 6733.
50. Tabandeh, F.; Khodabandeh, M.; Yakhchali, B.; Habib-Ghomi, H.; Shariati, P. *Chem. Eng. Sci.* **2008**, *63*, 2477.
51. Mirhosseini, H.; Tan, C. P.; Hamid, N. S. A.; Yusof, S. *J. Agric. Food Chem.* **2007**, *55*, 7659.
52. Peretto, G.; Du, W. X.; Avena-Bustillos, R. J.; Berrios, J. D. J.; Sambo, P.; McHugh, T. H. *J. Agric. Food Chem.* **2014**, *62*, 984.
53. Mayengbam, S.; Yang, H.; Barthet, V.; Aliani, M.; House, J. D. *J. Agric. Food Chem.* **2013**, *62*, 419.
54. Ahn, S. I.; Lee, Y. K.; Kwak, H. S. *J. Microencapsul.* **2013**, *30*, 460.
55. Aghbashlo, M.; Mobli, H.; Madadlou, A.; Rafiee, S. *J. Microencapsul.* **2012**, *29*, 790.
56. Arbia, W.; Adour, L.; Amrane, A.; Lounici, H. *Food Hydrocoll.* **2013**, *31*, 392.
57. Hosseinpour, V.; Kazemeini, M.; Mohammadrezaee, A. *Chem. Eng. Sci* **2011**, *66*, 4798.
58. Şahín, N.; Akoh, C. C.; Karaalí, A. *J. Agric. Food Chem.* **2006**, *54*, 3717.
59. Tsuda, N.; Ohtsubo, T.; Fuji, M. *Adv. Powder Technol.* **2012**, *23*, 724.
60. Han, Z. R.; Du, Y. C.; Li, G.; Mu, W.; Liu, F. *Chinese J. Pest. Sci.* **2007**, *9*, 405.
61. Ghadiri, M.; Fatemi, S.; Vatanara, A.; Doroud, D.; Najafabadi, A. R.; Darabiand, M.; Rahimi, A. A. *Int. J. Pharmaceut.* **2012**, *424*, 128.
62. Liu, J.; Chen, F.; Tian, W.; Ma, Y.; Li, J.; Zhao, G. *J. Agric. Food Chem.* **2014**, *62*, 7532.
63. McCarthy, E.; Flick, S.; Mérida, W. *J. Power Sources* **2013**, *239*, 399.
64. Li, B.; Wang, W.; Wang, K.; Zhang, D.; Guan, L.; Liu, F. *RSC Adv.* **2015**, *5*, 26654.
65. Zhou, Y.; Feng, J.; Zhang, X. *Chin. J. Pest. Sci* **2013**, *15*, 228.
66. Manca, D.; Rovaglio, M. *Chem. Eng. Sci.* **2003**, *58*, 1337.
67. He, Z.; Zhu, P. F.; Park, S. H. *Eur. J. Oper. Res.* **2012**, *221*, 241.
68. Heidari, H.; Razmi, H. *Talanta* **2012**, *99*, 13.